Published in final edited form as:
J Immunol. 2014 August 1; 193(3): 1162–1170. doi:10.4049/jimmunol.1303162.

mTOR complex 2 modulates αβT-cell receptor processing and surface expression during thymocyte development [1]

Po-Chien Chou[‡], **Won Jun Oh**[‡], **Chang-Chih Wu**[‡], **Joseph Moloughney**[‡], **Markus Rüegg**[§], **Michael N. Hall**[§], **Estela Jacinto**[‡,¶], and **Guy Werlen**[*,¶]

[*]Department of Cell Biology and Neuroscience, Rutgers, The State University of New Jersey, Piscataway, NJ 08854 [‡]Department of Biochemistry and Molecular Biology, Rutgers-Robert Wood Johnson Medical School, Piscataway, NJ 08854 [§]Biozentrum, University of Basel, CH 4056, Basel, Switzerland

Summary

An efficient immune response relies on the presence of T-cells expressing a functional T-cell receptor (TCR). While the mechanisms generating TCR diversity for antigenic recognition are well defined, what controls its surface expression is less known. Here we found that deletion of the mTORC2 component rictor at early stages of T-cell development led to aberrant maturation and increased proteasomal degradation of nascent TCR. While CD127 expression became elevated, the levels of TCR as well as CD4, CD8, CD69, Notch and CD147 were significantly attenuated on the surface of rictor-deficient thymocytes. Diminished expression of these receptors led to suboptimal signaling, partial DN4 proliferation and DP activation as well as developmental blocks at the double-negative 3 and CD8-ISP stages. Since CD147 glycosylation was also defective in SIN1-deficient fibroblasts, our findings suggest that mTORC2 is involved in the co/post-translational processing of membrane receptors. Thus, mTORC2 impacts development via regulation of the quantity and quality of receptors important for cell differentiation.

Keywords

glycosylation; mTORC2; post-translational processing; surface receptor; T-cell development

Introduction

The atypical protein kinase mTOR associates with various proteins to form two distinct protein complexes. mTOR complex 1 (mTORC1) is formed by mTOR, LST8 and raptor, while rictor, SIN1, LST8 and mTOR associate to form mTORC2. The mTORCs integrate environmental signals, including nutrients and growth factors, to promote cell growth and

[1]This work was supported by grants from the NIH (GM079176 and CA154674), Cancer Research Institute, Stand Up to Cancer Innovative Research Grant, Grant SU2C-AACR-IRG0311 (E.J.) Stand Up to Cancer is a program of the Entertainment Industry Foundation administered by the American Association for Cancer Research; New Jersey Commission for Cancer Research (08–1089-CCR-E0) and the Charles and Johanna Busch Memorial Fund at Rutgers, The State University of New Jersey (G.W.).

[¶]Correspondence: Guy Werlen, Tel. 908-655-1727, werlen@biology.rutgers.edu, Estela Jacinto, Tel. 732-235-4476, jacintes@rwjms.rutgers.edu.

differentiation (1, 2). Whereas mTORC1 mediates growth via its function in translation initiation and metabolism, mTORC2 is also emerging to play a role in these processes but the mechanisms remain to be elucidated (3, 4). mTOR complexes play a role in peripheral T-cell differentiation (5). mTORC2 was also recently shown to be involved in the early stages of T-cell ontogeny (6, 7) but the mechanisms as to how it controls these processes remain obscure.

Hematopoietic stem cells migrate from the bone marrow into the thymus where as immature thymocytes that do not yet express the coreceptors CD4 or CD8 ($CD4^{-}CD8^{-}$ double-negative; DN) they become committed to the T lymphocyte lineage that will express a polymorphic T-cell receptor (TCR) as hallmark (8–10) (Supplemental Fig. 1). The heterodimeric αβTCR composed of an α- and a β-chain associates with the invariant CD3 complex for surface expression and signaling. The β-chain is rearranged first in $CD25^{+}CD44^{-}$ DN3 cells and paired with an invariant pre-Tα-chain to form the pre-T-cell receptor (pre-TCR) (8–10). Although ligands for the pre-TCR remain unknown, its signaling is required for thymocyte survival and maturation at the β-selection checkpoint (8, 9). Thymocytes that successfully undergo β-selection downregulate CD25 and differentiate into DN4 ($CD25^{-}CD44^{-}$) cells (8, 9). These highly proliferating cells start expressing the CD8 coreceptor and differentiate into the transitional CD8-ISP (immature $CD8^{+}$ single positive) subsets that rearrange TCR-α chains and express a functional αβTCR (9, 11). The αβTCR as well as the CD8 and CD4 coreceptors are concomitantly expressed on the surface of $CD4^{+}CD8^{+}$ double-positive (DP) thymocytes that differentiate from CD8-ISP cells (9, 10). Only DP thymocytes expressing TCRs with appropriate affinities for self-peptide ligands go through positive selection and differentiate into $CD4^{+}CD8^{-}$ or $CD4^{-}CD8^{+}$ single positive (SP) thymocytes that egress the thymus and translocate to the peripheral lymphoid organs (9, 10). A number of studies have addressed the mechanisms generating TCR diversity for antigenic recognition as well as how downstream TCR-signaling components affect thymocyte differentiation to the CD8 or CD4 single-positive (SP) lineage (9, 10, 12). Much less is known about the mechanisms controlling receptor expression at the surface of thymocytes or T-cells.

Newly synthesized receptor polypeptides undergo post-translational modification in the ER including the addition of *N*-linked glycans, proper folding and in some cases such as the TCR, assembly of protein complexes (13). The oligosaccharides are then further trimmed and modified in the Golgi to form functional receptors with complex *N*-linked glycan structures. Nascent membrane and secretory proteins that fail to attain their final folded structure and fully mature in the ER and/or in the Golgi are destroyed by proteasomal degradation. How signaling molecules interact with and regulate protein processing in response to cellular conditions remains poorly understood particularly in higher eukaryotes. Here by deleting rictor during early thymocyte development, we report a novel function by which mTORC2 controls the expression of receptors that are relevant for T cell ontogeny, such as the pre-TCR and TCR as well as Notch, CD127 (α-chain of the Interleukin-7 receptor), CD147 (extracellular matrix metalloproteinase inducer), or the coreceptors, CD4 and CD8.

Materials and Methods

Mice and cell lines

Homozygous C56BL/6 *rictor*$^{f/f}$ mice (14) were crossed with C56BL/6 Lck-Cre mice (Taconic farms, NY), which generates T-cell-specific *rictor* knockout mice (rictor$^{T-/-}$) owing to the expression of Cre under the control of the proximal promoter of Lck. To specifically delete rictor in the OT-1 TCR background, we crossed C56BL/6/OT-1/β2m$^{-/-}$/Rag-2$^{-/-}$ mice (12) with homozygous rictor$^{T-/-}$ to obtain OT-1/Rag-2$^{-/-}$/rictor$^{T-/-}$ animals (referred to as OT-1/rictor$^{T-/-}$). All mice were genotyped by PCR using the respective primers described in Supplemental Table 1. Handling and experimentation protocols have been reviewed and used in accordance with IACUC regulations of Rutgers University. Tissues were removed from 6-week-old rictor$^{T-/-}$ and rictor$^{T+/+}$ littermates, micro-sliced and resuspended in RIPA buffer (50 mM Tris-HCl pH8.0, 100 mM NaCl, 5 mM EDTA, 1% Triton X-100, 0.2% SDS, 0.5% Na-deoxycholate supplemented with protease inhibitors). Jurkat cells were electroporated and transfected with rictor shRNA or scrambled shRNA (Invitrogen, CA). Transfected cells were cultured in complete RPMI medium in the presence of the selection antibiotic Zeocin (Invitrogen, CA). SIN1$^{-/-}$ MEFs cells were cultured as previously described (15).

Thymocyte proliferation and viability, immunostaining, and gene expression

Thymocytes were harvested in complete DMEM and counted by trypan blue exclusion. Cells were stained for receptor expression using antibodies listed in Supplemental Table 2. Stained cells were analyzed using a FACSCalibur flow cytometer and the CellQuest Pro (Becton Dickinson, NJ) or FlowJo (TreeStar, OR) software. Thymocytes were cultured in the presence of 100μM cycloheximide for the indicated times, followed by flow cytometric analysis to measure receptor turnover from the cell surface. Thymocytes were labeled with 2μM of CFSE (Sigma-Aldrich) prior to culturing in complete DMEM media at 37°C for 24 hrs. Cells were stained and cell division was analyzed on the flow cytometer by monitoring the shift in CFSE fluorescence. To assess cell viability, *ex vivo*-cultured thymocytes were stained with Annexin V (BD Pharmingen, CA) and propidium iodide (PI) (Sigma-Aldrich) prior to flow cytometric analysis. RNA was extracted from 1x10^7 thymocytes/point using the RNeasy kit (Qiagen, CA) and reverse transcribed by the iScript RT-PCR kit (Bio-Rad, CA) before amplification of cDNA templates using the respective primers described in Supplemental Table 1.

Thymocyte stimulation, lectin pull-down, immunoprecipitation, immunoblotting and *in vivo* labeling

Aliquots of 5x10^6 DP thymocytes were stimulated for various times with either 10 μg/ml CD3ε mAb (145–2C11), or 16 nM phorbol ester, PMA. Where indicated, cells were incubated for 4 hrs at 37°C in the presence of 50 μM MG132 (Tocris, MO), or its vehicle. Cells were stained for receptor surface expression, or lysed either in RIPA buffer or in 1 % Triton X-100 buffer (15 mM Tris-HCl, pH 7.5, 150 mM NaCl, 2 mM EDTA, supplemented with protease inhibitors). Proteins were resolved by SDS-PAGE and analyzed by immunoblotting using the antibodies listed in Supplemental Table 2. Where indicated, thymocyte or MEF lysates were incubated for 1 hr with 1500 Units of Endoglycosidase H or

PNGaseF (New England Biotechnology, MA). For lectin binding assays, we incubated 300 μg of thymocyte or MEF lysates overnight at 4°C with 20 μL of lectin-agaroses (Vector laboratories, CA), followed by washing with buffer containing 0.25% TX-100. Lysates or pull-down precipitates were run on SDS-PAGE followed by immunoblot analysis. For immuno-coprecipitation of mTORC2, $5x10^7$ wild-type or rictor-deficient thymocytes were harvested and lysed in 0.3% CHAPS buffer containing protease inhibitors (3) and proteins resolved as previously described (15). For [^{35}S] metabolic labeling experiments, $2x10^7$ thymocytes were incubated for 90 min at 37°C with methionine-free medium and then labeled for 30 min with 1 mCi/ml of [^{35}S]-methionine (Perkin-Elmer, MA). After labeling, cells were replaced with normal DMEM medium containing 5 mM methionine/cysteine and incubated for the indicated "chase" times. Cells were lysed in RIPA buffer and TCRα-chains were immunoprecipitated overnight at 4°C. SDS-PAGE-resolved proteins were transferred onto a PVDF membrane and the incorporation of [^{35}S] was assessed by autoradiography followed by immunoblotting for TCRα and ubiquitin. Densitometric analysis of protein expression, or postranslational phosphorylation was performed using the Image J software from NIH.

Results

Rictor deficiency in the thymus led to a marked decrease in thymocyte number and partial differentiation blocks at the DN3 and CD8-ISP stages

By gene ablation, we generated the rictor$^{T-/-}$ mouse model in which rictor expression (Fig. 1A) and mTORC2 assembly (Fig. 1B) was exclusively disrupted in T-cells starting at the DN2 stage of thymocyte development (Supplemental Fig. 1). While T-cell-specific ablation of *rictor* had no effect on size, viability and reproduction of rictor$^{T-/-}$ mice (data not shown), it dramatically affected the number of thymocytes in these animals (Fig. 1C). As thymopoiesis fluctuates during the lifespan of an individual, thymocytes from different age groups ranging from e15 embryos to 6-week-old mice were analyzed (Fig. 1D). While *rictor* ablation diminished the number of thymocytes by 25% in embryos, it led to a 50% reduction in 1-week-old rictor$^{T-/-}$ mice as compared to rictor$^{T+/+}$ littermates and a massive cell loss of up to 80% in 3-6 week old knockout animals (Fig. 1D). This age-associated thymocyte decline suggests that rictor plays an essential role in the generation or homeostasis of these cells. As previously reported (6, 7), we also found a stage-specific developmental block that could account for the severe thymocyte loss in rictor$^{T-/-}$ mice (data not shown). A pronounced increase in the CD25$^+$CD44$^-$ (DN3) population was accompanied by a striking attenuation of DN4 (CD25$^-$CD44$^-$) cells (Fig. 1E), suggesting that rictor is required for DN3 to DN4 differentiation. Concomitantly, a modest elevation of the absolute number of rictor-deficient DN3 thymocytes was associated with a dramatic decrease in DN4 cells (Fig. 1F), implying that a defective β-selection checkpoint probably accounted for delayed maturation to this stage.

Additionally, the absence of rictor could further obstruct thymocyte development by impacting the DN4 to CD8-ISP transition. Among the cells bearing the coreceptor CD8, but not CD4, we found 20% CD8-ISPs (TCR^{low}, CD8$^+$, CD147$^+$, CD4$^-$, CD127$^-$) that also prominently expressed the extracellular matrix metalloproteinase inducer, CD147 (9, 11)

and 80% mature SP (TCR^{high}, $CD8^+$, $CD127^+$, $CD4^-$, $CD147^-$) cells that express the α-chain of the Interleukin-7 receptor, CD127 instead of CD147 (Fig. 1G). However, in $rictor^{T-/-}$ mice the proportions were reversed resulting in a substantial increase in the relative and absolute number of CD8-ISP cells (Fig. 1G). Interestingly, the relative numbers of CD8-ISP were similar in wild-type and rictor-deficient e15 embryos, while the difference increased after birth to reach a ~ 4-fold greater proportion in 4-week-old $rictor^{T-/-}$ mice as compared to the wild-type littermates (Fig. 1H). Thus, defective mTORC2 triggered a partial developmental block at the CD8-ISP stage that was exacerbated with age and could, together with delayed DN3 to DN4 differentiation, explain the pronounced reduction in thymocytes.

Cell surface expression of receptors relevant for thymocyte development was defective in absence of rictor

We noticed that while $rictor^{T-/-}$ newborns expressed slightly less CD147 on the surface of CD8-ISPs as compared to wild-type cells, about 40% less of this membrane glycoprotein was found on CD8-ISP thymocytes of 4-week-old $rictor^{T-/-}$ mice (Fig. 2A). Similarly, in absence of rictor, CD8 expression was significantly reduced on the surface of mature CD8-SP cells (Fig. 2B), while CD127 was in contrast upregulated on these cells (Fig. 2C). In accordance with a role of mTORC2 in Notch-driven thymocyte differentiation (7), the surface expression of Notch was also consistently decreased on rictor-ablated thymocytes (Fig. 2D). Furthermore, significantly diminished expression of pre-TCR or TCR was observed in absence of rictor at each of the respective stages wherein they affect thymocyte development (Fig. 2E). This attenuation became particularly pronounced at later (DP and SP) stages and seemed to persist beyond T-cell maturation in the thymus, as we also observed it on rictor-deficient peripheral T-cells (Supplemental Fig. 2A). CD8 and CD4 expression was also significantly diminished on the surface of rictor-deficient DP and SP cells (Fig. 2B and 2F) as well as peripheral T-cells (Supplemental Fig. 2A). Overall, our results suggest that mTORC2 could play a role in controlling the expression of receptors relevant for T cell ontogeny.

Decreased pre-TCR or TCR expression resulted in suboptimal signaling and cell responses in absence of rictor

Among developing thymocytes, DN4 cells are the main population undergoing proliferation and although ligands for the pre-TCR remain unknown, its surface expression is required for DN4 clonal expansion (8, 9, 16). Thus, we asked if decreased pre-TCR expression would affect the division of rictor-deficient DN4 cells and consequently partially account for their reduced cell number. We labeled wild-type and rictor-deficient thymocytes with the fluorescent dye CFSE and assessed proliferation by flow cytometry after 24h of cell culture. As expected, neither DP nor SP cells spontaneously divided (data not shown), however, 37% of wild-type DN4 thymocytes but only 17% of rictor-deficient counterparts accomplished at least one division in 24h (Fig. 3A). Both the surface expression of CD147 and the relative number of DN4 cells expressing this marker of cell proliferation was significantly decreased in absence of rictor as compared to its presence (Fig. 3B), supporting a defect in the cell cycling machinery in those cells. While the addition of CD3ε mAb in the culture media further increased the percentage of dividing wild-type DN4 thymocytes it had

no effect on rictor-deficient counterparts (Fig. 3A), suggesting that the reduced pre-TCR surface expression accounted in part for defective DN4 clonal expansion in rictor$^{T-/-}$ mice. To further assess the consequence of lower receptor expression, we measured the TCR-dependent expression of CD69, a marker for T-cell activation (17). CD3ε mAb was markedly less potent in triggering CD69 expression on rictor-deficient thymocytes as compared to wild-type cells. Indeed, both the relative number of CD69-positive cells (CD69^{+}) as well as the surface amount of this receptor were significantly reduced in absence of rictor (Fig. 3C & 3D), corroborating that lower TCR levels affected the functionality of rictor$^{T-/-}$ thymocytes by probably delaying the transduction of required intracellular signals.

To test the latter, we examined the phosphorylation of ERK, a kinase essential for CD69 expression (17) and thymocyte differentiation (12) that is activated by TCR-engagement. Compared to wild-type cells, ERK phosphorylation was markedly reduced following CD3ε mAb stimulation of rictor-deficient thymocytes (Fig. 4A). In contrast, the addition of PMA led to maximal phosphorylation of ERK after 10 min of stimulation (Fig. 4B), as well as to the expression of CD69 in most thymocytes after 6 hrs of treatment (Fig. 3C), independently of the presence or absence of a functional mTORC2 complex. These results indicated that the abrogation of *rictor* only affected the activation of ERK and consequently CD69 expression in response to TCR engagement, but not to stimuli that bypass the receptor. In contrast, both anti-CD3ε mAb and PMA treatment induced significantly less CD69 on the surface of rictor$^{T-/-}$ thymocytes as compared to rictor$^{T+/+}$ cells (Fig. 3D), supporting a defect in the molecular mechanisms controlling CD69 expression in absence of rictor. The activation of Akt was also affected in rictor-deficient cells following TCR-engagement (Fig. 4A). While, the loss of rictor completely abolished the phosphorylation of Akt at both mTORC2 target sites, Ser473 (hydrophobic motif; HM) and Thr450 (turn motif; TM) (Fig. 4B and C), anti-CD3ε mAb only marginally rescued this phosphorylation (Fig. 4A) and PMA treatment had no effect whatsoever (Fig. 4B). Concomitantly, the Akt substrate, FoxO1 was hypophosphorylated in rictor-deficient thymocyte (Fig. 4C), even following PMA stimulation (Fig. 4B). Similarly, the loss of mTORC2 accounted for diminished HM site phosphorylation of another AGC kinase, PKCα that could also not be rescued by PMA stimulation of rictor$^{T-/-}$ thymocytes (Fig. 3B and 3C), suggesting that rictor ablation broadly affected signaling in those cells. However, despite marked defects in Akt signaling in absence of mTORC2 (Fig. 4A-C), there was no significant changes in overall cell viability (Fig. 4D) as well as viability of particular rictor-deficient thymocyte subsets (data not shown). In addition, there was no significant alteration in the phosphorylation of the mTORC1 targets S6 and ULK1 (Fig. 4C and Supplemental Fig. 2B), nor in the expression of the autophagy effector LC3-II (Fig. 4C), suggesting that the ablation of *rictor* specifically affected the phosphorylation of mTORC2 substrates and effectors, but not mTORC1 activity or autophagy. Together, our results reveal a partially defective signaling in mTORC2-disrupted cells due to decreased surface expression of relevant receptors including the pre-TCR or TCR that affected cell responses such as proliferation, as well as decreased CD147 and CD69 surface expression.

Defective processing of newly synthesized polypeptides accounted for reduced TCR levels in absence of rictor

We then examined how mTORC2 can affect TCR surface expression. Whereas abrogating rictor almost doubled the transcription of CD127, it did not affect the levels of TCRα, TCRβ, and CD3ε mRNAs (Fig. 5A), indicating that defective gene expression unlikely accounted for the diminished levels of αβTCR on the surface of rictor$^{T-/-}$ thymocytes. A higher rate of endocytosis could lead to defective receptor expression even in absence of ligand stimulation, as reported recently for the TCR (18). However in presence of cycloheximide, the TCR, CD4 and CD8 turnover from the surface of rictor-deficient thymocytes were unchanged or slightly slower as compared to wild-type cells (Fig. 5B and data not shown), indicating that increased endocytosis was unlikely responsible for the reduced receptor expression in absence of rictor. Thus, we considered whether rictor deficiency might alter *de novo* synthesis of the TCR complex. To facilitate biochemical analysis of the TCRα- or β-chains that, in contrast to CD3ε were present in meager amounts in whole cell extracts of rictor-deficient thymocytes (Fig. 5C, lane 1 vs 2 and data not shown), we crossed transgenic mice expressing exclusively the Vα2, TCRα- and Vβ5, TCRβ-chains (OT-1 TCR) (12) onto the rictor-deficient background (OT-1/rictor$^{T-/-}$ mice). Compared to wild-type OT-1 cells, significantly less OT-1 TCR was also found on the surface of OT-1/rictor$^{T-/-}$ thymocytes, as measured by Vα2 expression (Fig. 5D). Nevertheless, sufficient amounts of Vα2 could now be obtained by immunoprecipitation from rictor-deficient cells to allow examining the synthesis of this TCR-α chain (Fig. 5E, middle panel). After [^{35}S]-methionine labeling, the level of the radioactive Vα2 band (MW~38 kD) gradually decreased over time in wild-type thymocytes (Fig. 5E, **x** symbol, lane 1-4, upper panel), while it was barely discernible in rictor-deficient cells after 1 h of chase (Fig. 5E, lane 6-8, upper panel). Instead, a faster migrating band of ~29kDa that likely corresponded to the native TCRα polypeptide lacking *N*-linked oligosaccharides and *N*-terminal signal peptide (19) accumulated in those thymocytes (Fig. 5E, arrow lane 5-8, upper panel). These results suggest increased misprocessing of de novo synthesized TCRα-chains in absence of rictor. In support, there was augmented ubiquitylation of Vα2-chains (Ubi-TCRα) in OT-1/rictor$^{T-/-}$ cell lysates (Fig. 5E, lane 6-8, lower panel). Furthermore, treating rictor-deficient thymocytes with the proteasome inhibitor MG132 enhanced TCRα and TCRβ expression in whole cell lysate by almost 4-fold compared to only 2-fold for wild-type cells (Fig. 5C, lane 2 vs 4 and data not shown) In contrast, TCR surface expression was unaffected by the addition of MG132 in the cell culture prior to flow cytometric analysis (Supplemental Fig. 2C). Overall, our results support a role for mTORC2 in the processing and maturation of TCR-chains.

Next, we used lectin pull-down assays to examine whether defective TCR-α glycosylation caused receptor misprocessing in absence of rictor. The lectin Sambucus nigra (SNA) that recognizes terminal sialic acid residues of complex *N*-glycan moieties (13) bound similar amounts of TCR-α from wild-type and rictor-deficient thymocytes (Fig. 5F, lane 5 vs 6 upper panel). Thus, a defect in this late glycan modification could not account for enhanced TCR misprocessing in absence of rictor. Indeed, SNA did not bind more receptor following MG132-treatment (Fig. 5F, lane 6 vs 8 upper panel), despite a 4-fold increase in TCR-α expression (Fig. 5F, lane 2 vs 4 upper panel). We then used Galanthus nivalis lectin (GNL),

which binds to α-1,3-mannose residues that are generated at early steps of *N*-glycan trimming. GNL bound quite comparable amounts of TCR α-chains from MG132-treated and non-treated wild-type thymocytes (Fig. 5F, lane 5 vs 7, lower panel). In contrast, GNL was about 3-times more efficient in binding TCR-α from inhibitor-treated rictor-deficient cells as compared to non-treated counterparts (Fig. 5F, lane 6 vs 8 lower panel), indicating a partially defective receptor-glycosylation in absence of rictor that markedly augmented TCR-α misprocessing and proteosomal degradation. This defect likely occurs either in the cis- or medial-Golgi during the early steps of protein glycosylation.

mTORC2 disruption or inhibition deregulates the expression of CD147 in immortalized T-cells as well as mouse embryonic fibroblasts (MEFs)

Since CD147 expression was reduced on the surface of rictor-deficient thymocytes (Fig. 2A and 3B), but in contrary to the TCR, this receptor is ubiquitously expressed on proliferating cells (20), we used it as a model to further examine the role of mTORC2 in receptor glycosylation and processing. The level of CD147 was significantly diminished on the surface of SIN1-deficient MEFs (Fig. 6A), as compared to wild-type cells in which mTORC2 is not disrupted (15). Interestingly, in contrast to wild-type MEFs, the high glycosylated (HG) form of CD147 was hardly detectable in $SIN1^{-/-}$ cell extracts and the majority of this protein displayed a faster electrophoretic migration (Fig. 6B, lane 1 vs 4), suggesting that it could be improperly glycosylated in the latter cells. Indeed, while CD147 from wild-type MEF extracts was insensitive to EndoH, the low glycosylated (LG) CD147 from $SIN1^{-/-}$ MEFs further collapsed into a < 30 kDa polypeptide (Fig. 6B, lane 2 vs 5). This faster migrating protein corresponded to the fully deglycosylated form of CD147, as revealed by treatment with the glycosidase PNGase F (Fig. 6B, lane 3 vs 5 & 6). Again, we used the lectin pull-down assay to analyze the *N*-glycan modifications present on CD147 from wild-type and $SIN1^{-/-}$ cells, but this time we used GNL as well as, Leucoagglutinin Phaseolus vulgaris (L-PHA) and Griffonia simplicifolia II (GSL-II). The latter two lectins recognize sugar moieties that are conjugated to complex glycan structures at more distal steps along the trans/medial Golgi than the mannose bound by GNL (13). While all 3 lectins potently bound to high-glycosylated (HG) CD147 in wild-type MEFs (Fig. 6C, HG in lane 3, 5 & 7), only GNL associated substantially to LG CD147 in these cells (Fig. 6C, LG in lane 7). In contrast, L-PHA and GSL-ll pulled-down very little to no CD147 from $SIN1^{-/-}$ extracts (Fig. 6C, lane 4 & 6) while, GNL bound the majority of this receptor (Fig. 6C, lane 8), implying that most of the CD147 in these cells contained α-1,3 mannose residues, but not more complex glycan structures. These results indicate a partial CD147-glycosylation defect in absence of SIN1, at an early step of glycan maturation. In addition, they concur with our findings documenting a defective TCR-glycosylation in rictor-ablated thymocytes and further support an involvement of mTORC2 in the early steps of receptor glycosylation and processing.

Lastly, as the expression of CD147 has been found elevated in a number of tumors, including T-cell lymphoid leukemia (T-ALL) (21, 22), we examined whether its levels on the surface of the T-cell line, Jurkat, correlated with augmented mTORC2 activity. Compared to both non-transformed peripheral T-cells and thymocytes, Jurkat cells bear a tremendously higher phosphorylation of mTOR and Akt's HM (Fig. 6D, lane 2 vs 3 & 4)

that was associated with a dramatic increase of CD147 surface expression (Fig. 6E). Indeed, knocking down rictor (Fig. 6D, lane 1 vs 2) or blocking the activity of mTORC2 (Supplemental Fig. 2D), significantly reduced the expression of CD147 on the surface of Jurkat cells. Thus, besides controlling the processing of receptors relevant for T-cell ontogeny, mTORC2 controlled the surface expression of CD147 in a variety of cells.

Discussion

Our findings of a partial block of thymocyte development at the DN3 stage concur with previous reports documenting the disruption of mTORC2 in T cells (6, 7). Importantly, we reveal for the first time that mTORC2 could control cell responses by regulating the levels of critical plasma membrane receptors that drive specific stages of cell development or proliferation. By controlling the amounts of surface receptors, mTORC2 would optimize the transduction of signals required for cell fate decisions. Among the many receptors relevant for early thymocyte development, the reduced pre-TCR/TCR levels (Fig. 2E) could account for decreased DN4 proliferation (Fig. 3A) and together with the decreased Notch and CD147 expression (Fig. 2A, 2D and 3B) could delay maturation to the DP stage, even in presence of increased expression of CD127 (Fig. 2C and 5A). Additionally, diminished TCR as well as CD4 and CD8 expression on DP thymocytes (Fig. 2B and Fig. 2E-F) generated suboptimal signaling (Fig. 4A) leading to delayed activation and maturation to the SP stage (Fig. 3C). Furthermore, reduced TCR as well as CD4 or CD8 levels (Supplemental Fig. 2A) could impact homeostasis of peripheral rictor-deficient T-cells, even in the presence of increased levels of cytokine receptors such as CD127 and explain in part some of the changes in peripheral T cell differentiation previously reported (5). Thus, overall abnormal expression of relevant receptors could account for most of the T-cell specific developmental defects that we have documented here upon rictor deletion.

How mTORC2 can regulate receptor surface expression remains to be elucidated, but our findings suggest that this complex accounted for the observed defects rather than a global change in mTOR signaling. Indeed, while mTORC1 signaling involving S6K and S6 was not diminished in rictor-deficient thymocytes (Fig. 4C and Supplemental Fig. 2B), autophagy was not impaired either by the ablation of *rictor* as indicated by normal LC3-II levels and ULK1 phosphorylation (Fig. 4C). Instead, specific mTORC2 targets and downstream effectors such as the AGC kinases, Akt and PKCα/β as well as the Akt-effector, Fox01/3 have defective phosphorylation and signaling in rictor-deficient thymocytes (Fig. 4A-C). Whereas the transcription factor Foxo1 has previously been reported to control the expression of CD127 (23, 24), mTORC2 could contribute to this transcriptional mechanism by regulating the phosphorylation of Akt. Therefore, defective phosphorylation of Akt and FoxO1 could account for the augmented transcription and surface expression of CD127 that we observe in rictor$^{T-/-}$ mice (Fig. 2C and 5A). Notably while required for T-cell ontogeny as well as peripheral homeostasis (25), enhanced CD127 was not able to compensate for the developmental defects observed in rictor-deficient thymocytes. In contrast and while the mechanism would remain to be investigated, CD127 might have contributed to preserve the viability of rictor$^{T-/-}$ cells (Fig. 4D) even in presence of markedly defective Akt signaling (Fig. 4A-C). Nonetheless, most receptor we examined were decreased, not increased, on the surface of rictor-deficient thymocytes, indicating that mTORC2 could impinge on various

molecular mechanisms that would each specifically modulate the levels of particular membrane receptors. For instance, while CD127 was increased on the surface of rictor-deficient cells, it might also potentially be affected by a similar postranslational defect as the rest of the receptors examined. Indeed, an almost 2-fold augmented CD127 transcript in rictor$^{T-/-}$ cells (Fig. 4A) resulted in only a ~30% increase in receptor surface level (Fig. 2C), implying that some CD127 was lost after transcription. Furthermore, as compared to wild-type cells, CD69 was less upregulated on the surface of rictor-deficient DP thymocytes in response to both anti-CD3ε mAb and PMA (Fig. 3D), despite the latter treatment triggering full activation of ERK (Fig. 4B), a signaling cascade required for maximal expression of CD69 (17). Interestingly, the kinetics of ERK activation were quite different in anti-CD3ε mAb stimulated rictor$^{T-/-}$ and rictor$^{T+/+}$ thymocytes (Fig. 4A). A fast and somewhat transient ERK phosphorylation was observed in wild-type cells, while the activation of this kinase was slow but sustained in absence of rictor (Fig. 4A, right panel). This result was reminiscent of the signature ERK kinetics that we have documented previously in response to ligands inducing either differentiation or death of activated DP thymocytes (12). Whether the abrogation of *rictor* affects thymic selection, owing to reduced TCR expression and ensuing signaling defects remains to be investigated. Nonetheless, while our results provided indirect evidence, the literature adds credibility to this possibility. Indeed, disrupting mTORC2 in mature T cells affects T helper cell differentiation (26). While, AGC kinase signaling was defective in these mice, complementation with either active Akt or PKC-θ rescued Th1 and Th2 differentiation, respectively (26). Defective TCR surface expression was not explicitly accounted for in this report, or any other report published so far discussing T-cell-targeted rictor or AGC kinase mouse models, including Akt null mice (27–29). It would thus also be interesting to determine if altered amounts of TCR and/or cytokine receptors critical for the generation of Th1 and Th2 accounted in part, for the defects reported in the literature by Lee et al (26). Nevertheless, while we cannot exclude that several mTORC2-dependent AGC kinases cooperate to control receptor expression, our new findings support a role for mTORC2 in the processing of nascent receptor polypeptides and more precisely during their early glycosylation steps. Notably, the loss of rictor decreased the expression of *N*-glycosylated α- and β-chains of the TCR, but not CD3ε, the non-glycosylated component of the TCR/CD3 complex (Fig. 5C and data not shown). CD147, another highly glycosylated receptor had decreased expression in DN4 and CD8-ISP thymocytes as well as MEFs and was misprocessed in the latter cells. Interestingly, CD147 has been recently implicated in the maturation of lactate transporters at the plasma membrane of proliferative cells undergoing enhanced glycolysis (30, 31). Thus, defective CD147 surface expression in absence of rictor could possibly impact cell division due to its role in glycolytic metabolism and consequently, protein glycosylation. Notably, altered *N*-glycosylation of growth factor receptors has previously been correlated with deregulated cell proliferation as well as defective Akt signaling (32, 33). Whether Akt could also modulate glycan maturation in the Golgi is a possibility considering previously documented involvement of this kinase in controlling indirectly glycosylation via the ER enzyme, ENTPD5 (32). There is also accumulating evidence that mTORC2 plays a role in metabolic and biosynthetic pathways (34, 35). Whether it is involved in the generation of metabolic intermediates crucial for the process of protein glycosylation remains to be investigated. Finally, since altered surface

expression of mitogenic receptors plays a role in defective proliferation or differentiation of a number of cells, our studies provide rationale for specifically targeting mTORC2 in developing new treatments to prevent the onset or progression of various diseases including malignancies and T-cell-derived disorders.

Supplementary Material

Refer to Web version on PubMed Central for supplementary material.

Acknowledgments

We thank Drs. L. Covey, A. Laouar, and A. Rabson for critical reading of the manuscript.

References

1. Jewell JL, Guan KL. Nutrient signaling to mTOR and cell growth. Trends Biochem Sci. 2013; 38:233–242. [PubMed: 23465396]
2. Yang K, Chi H. mTOR and metabolic pathways in T cell quiescence and functional activation. Semin Immunol. 2012; 24:421–428. [PubMed: 23375549]
3. Oh WJ, Wu CC, Kim SJ, Facchinetti V, Julien LA, Finlan M, Roux PP, Su B, Jacinto E. mTORC2 can associate with ribosomes to promote cotranslational phosphorylation and stability of nascent Akt polypeptide. Embo J. 2010; 29:3939–3951. [PubMed: 21045808]
4. Dai N, Christiansen J, Nielsen FC, Avruch J. mTOR complex 2 phosphorylates IMP1 cotranslationally to promote IGF2 production and the proliferation of mouse embryonic fibroblasts. Genes Dev. 2013; 27:301–312. [PubMed: 23388827]
5. Waickman AT, Powell JD. mTOR, metabolism, and the regulation of Tcell differentiation and function. Immunol Rev. 2012; 249:43–58. [PubMed: 22889214]
6. Tang F, Wu Q, Ikenoue T, Guan KL, Liu Y, Zheng P. A critical role for Rictor in T lymphopoiesis. J Immunol. 2012; 189:1850–1857. [PubMed: 22815285]
7. Lee K, Nam KT, Cho SH, Gudapati P, Hwang Y, Park DS, Potter R, Chen J, Volanakis E, Boothby M. Vital roles of mTOR complex 2 in Notch-driven thymocyte differentiation and leukemia. J Exp Med. 2012; 209:713–728. [PubMed: 22473959]
8. Bhandoola A, von Boehmer H, Petrie HT, Zuniga-Pflucker JC. Commitment and developmental potential of extrathymic and intrathymic T cell precursors: plenty to choose from. Immunity. 2007; 26:678–689. [PubMed: 17582341]
9. Germain RN. T-cell development and the CD4-CD8 lineage decision. Nat Rev Immunol. 2002; 2:309–322. [PubMed: 12033737]
10. Werlen G, Hausmann B, Naeher D, Palmer E. Signaling life and death in the thymus: timing is everything. Science. 2003; 299:1859–1863. [PubMed: 12649474]
11. Renno T, Wilson A, Dunkel C, Coste I, Maisnier-Patin K, Benoit de Coignac A, Aubry JP, Lees RK, Bonnefoy JY, MacDonald HR, Gauchat JF. A role for CD147 in thymic development. J Immunol. 2002; 168:4946–4950. [PubMed: 11994445]
12. Werlen G, Hausmann B, Palmer E. A motif in the alphabeta T-cell receptor controls positive selection by modulating ERK activity. Nature. 2000; 406:422–426. [PubMed: 10935640]
13. Dennis JW, Nabi IR, Demetriou M. Metabolism, cell surface organization, and disease. Cell. 2009; 139:1229–1241. [PubMed: 20064370]
14. Bentzinger CF, Romanino K, Cloetta D, Lin S, Mascarenhas JB, Oliveri F, Xia J, Casanova E, Costa CF, Brink M, Zorzato F, Hall MN, Ruegg MA. Skeletal muscle-specific ablation of raptor, but not of rictor, causes metabolic changes and results in muscle dystrophy. Cell Metab. 2008; 8:411–424. [PubMed: 19046572]
15. Jacinto E, Facchinetti V, Liu D, Soto N, Wei S, Jung SY, Huang Q, Qin J, Su B. SIN1/MIP1 Maintains rictor-mTOR Complex Integrity and Regulates Akt Phosphorylation and Substrate Specificity. Cell. 2006; 127:125–137. [PubMed: 16962653]

16. Michie AM, Zuniga-Pflucker JC. Regulation of thymocyte differentiation: pre-TCR signals and beta-selection. Semin Immunol. 2002; 14:311–323. [PubMed: 12220932]
17. D'Ambrosio D, Cantrell DA, Frati L, Santoni A, Testi R. Involvement of p21ras activation in T cell CD69 expression. Eur J Immunol. 1994; 24:616–620. [PubMed: 7907294]
18. Wang H, Holst J, Woo SR, Guy C, Bettini M, Wang Y, Shafer A, Naramura M, Mingueneau M, Dragone LL, Hayes SM, Malissen B, Band H, Vignali DA. Tonic ubiquitylation controls T-cell receptor:CD3 complex expression during T-cell development. Embo J. 2010; 29:1285–1298. [PubMed: 20150895]
19. Yu H, Kaung G, Kobayashi S, Kopito RR. Cytosolic degradation of T-cell receptor alpha chains by the proteasome. J Biol Chem. 1997; 272:20800–20804. [PubMed: 9252404]
20. Gabison EE, Hoang-Xuan T, Mauviel A, Menashi S. EMMPRIN/CD147, an MMP modulator in cancer, development and tissue repair. Biochimie. 2005; 87:361–368. [PubMed: 15781323]
21. Chen X, Su J, Chang J, Kanekura T, Li J, Kuang YH, Peng S, Yang F, Lu H, Zhang JL. Inhibition of CD147 gene expression via RNA interference reduces tumor cell proliferation, activation, adhesion, and migration activity in the human Jurkat T-lymphoma cell line. Cancer Invest. 2008; 26:689–697. [PubMed: 18608214]
22. Nabeshima K, Suzumiya J, Nagano M, Ohshima K, Toole BP, Tamura K, Iwasaki H, Kikuchi M. Emmprin, a cell surface inducer of matrix metalloproteinases (MMPs), is expressed in T-cell lymphomas. J Pathol. 2004; 202:341–351. [PubMed: 14991900]
23. Kerdiles YM, Beisner DR, Tinoco R, Dejean AS, Castrillon DH, DePinho RA, Hedrick SM. Foxo1 links homing and survival of naive T cells by regulating L-selectin, CCR7 and interleukin 7 receptor. Nat Immunol. 2009; 10:176–184. [PubMed: 19136962]
24. Ouyang W, Beckett O, Flavell RA, Li MO. An essential role of the Forkhead-box transcription factor Foxo1 in control of T cell homeostasis and tolerance. Immunity. 2009; 30:358–371. [PubMed: 19285438]
25. Carrette F, Surh CD. IL-7 signaling and CD127 receptor regulation in the control of T cell homeostasis. Semin Immunol. 2012; 24:209–217. [PubMed: 22551764]
26. Lee K, Gudapati P, Dragovic S, Spencer C, Joyce S, Killeen N, Magnuson MA, Boothby M. Mammalian target of rapamycin protein complex 2 regulates differentiation of Th1 and Th2 cell subsets via distinct signaling pathways. Immunity. 2010; 32:743–753. [PubMed: 20620941]
27. Mao C, Tili EG, Dose M, Haks MC, Bear SE, Maroulakou I, Horie K, Gaitanaris GA, Fidanza V, Ludwig T, Wiest DL, Gounari F, Tsichlis PN. Unequal contribution of Akt isoforms in the double-negative to double-positive thymocyte transition. J Immunol. 2007; 178:5443–5453. [PubMed: 17442925]
28. Juntilla MM, Wofford JA, Birnbaum MJ, Rathmell JC, Koretzky GA. Akt1 and Akt2 are required for alphabeta thymocyte survival and differentiation. Proc Natl Acad Sci U S A. 2007; 104:12105–12110. [PubMed: 17609365]
29. Hinton HJ, Alessi DR, Cantrell DA. The serine kinase phosphoinositidedependent kinase 1 (PDK1) regulates T cell development. Nat Immunol. 2004; 5:539–545. [PubMed: 15077109]
30. Kirk P, Wilson MC, Heddle C, Brown MH, Barclay AN, Halestrap AP. CD147 is tightly associated with lactate transporters MCT1 and MCT4 and facilitates their cell surface expression. Embo J. 2000; 19:3896–3904. [PubMed: 10921872]
31. Le Floch R, Chiche J, Marchiq I, Naiken T, Ilk K, Murray CM, Critchlow SE, Roux D, Simon MP, Pouyssegur J. CD147 subunit of lactate/H+ symporters MCT1 and hypoxia-inducible MCT4 is critical for energetics and growth of glycolytic tumors. Proc Natl Acad Sci U S A. 2011; 108:16663–16668. [PubMed: 21930917]
32. Fang M, Shen Z, Huang S, Zhao L, Chen S, Mak TW, Wang X. The ER UDPase ENTPD5 promotes protein N-glycosylation, the Warburg effect, and proliferation in the PTEN pathway. Cell. 2010; 143:711–724. [PubMed: 21074248]
33. Lau KS, Partridge EA, Grigorian A, Silvescu CI, Reinhold VN, Demetriou M, Dennis JW. Complex N-glycan number and degree of branching cooperate to regulate cell proliferation and differentiation. Cell. 2007; 129:123–134. [PubMed: 17418791]

34. Hagiwara A, Cornu M, Cybulski N, Polak P, Betz C, Trapani F, Terracciano L, Heim MH, Ruegg MA, Hall MN. Hepatic mTORC2 Activates Glycolysis and Lipogenesis through Akt, Glucokinase, and SREBP1c. Cell Metab. 2012; 15:725–738. [PubMed: 22521878]

35. Masui K, Tanaka K, Akhavan D, Babic I, Gini B, Matsutani T, Iwanami A, Liu F, Villa GR, Gu Y, Campos C, Zhu S, Yang H, Yong WH, Cloughesy TF, Mellinghoff IK, Cavenee WK, Shaw RJ, Mischel PS. mTOR complex 2 controls glycolytic metabolism in glioblastoma through FoxO acetylation and upregulation of c-Myc. Cell Metab. 2013; 18:726–739. [PubMed: 24140020]

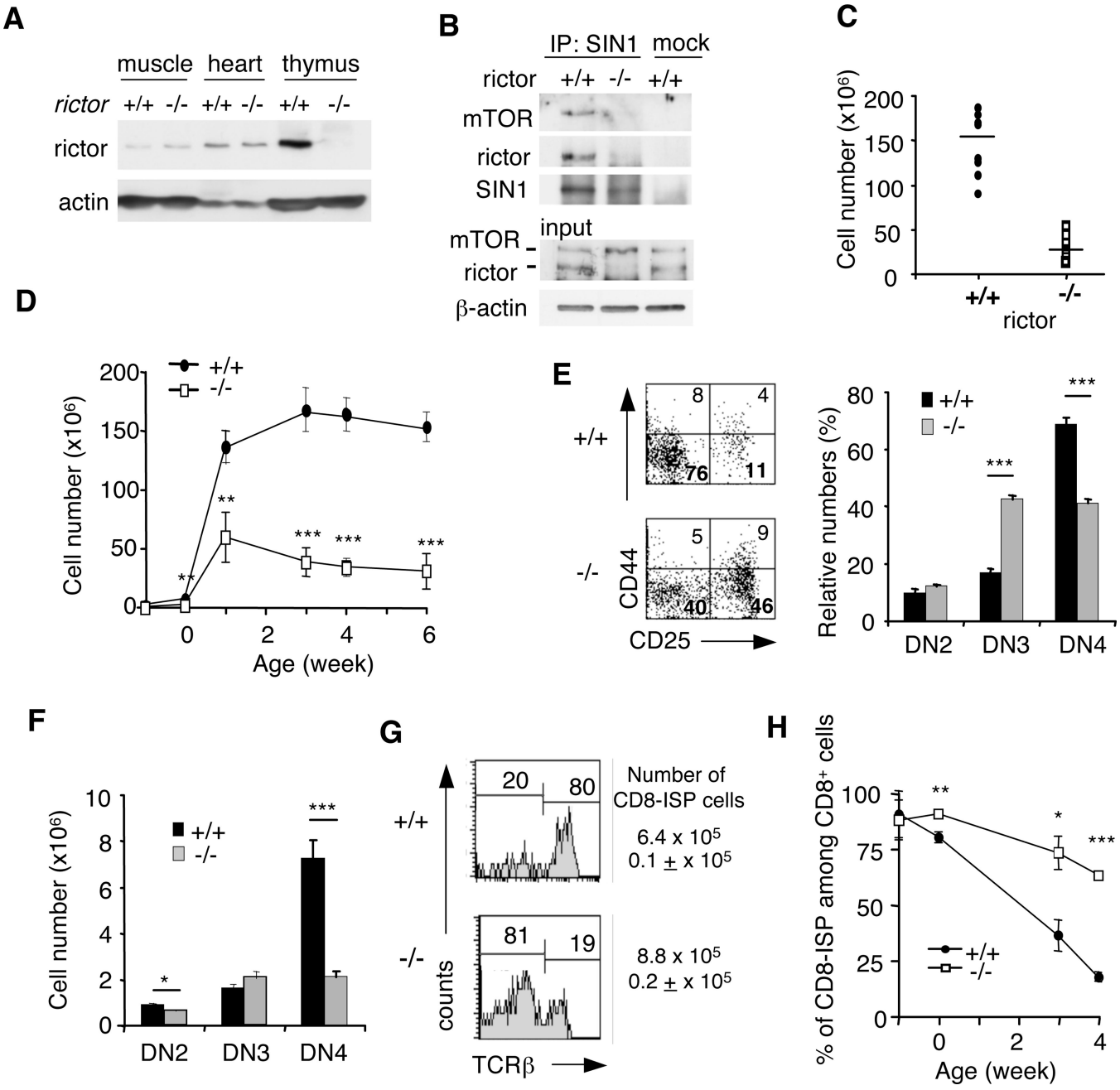

Fig. 1. Targeted *rictor* ablation decreased the number of thymocytes and led to partial differentiation blocks at the DN3 and CD8-ISP stages

A. Thymocyte lysates from wild-type (+/+) or rictor$^{T-/-}$ (−/−) littermates were resolved by SDS-PAGE and analyzed by immunoblotting. Shown is a representative experiment out of two. **B**. SIN1 was immunoprecipitated from wild-type (+/+) or rictor$^{T-/-}$ (−/−) thymocyte lysates and associated mTOR or rictor was analyzed by immunoblotting (mk: mock IP). Shown is a representative experiment out of three. **C.** Thymocytes from 6-week-old rictor$^{T+/+}$ and rictor$^{T-/-}$ littermates were harvested and counted. Each symbol represents one mouse (n=10). Bars indicate mean values. **D.** Thymocytes from age-matched rictor$^{T+/+}$ and rictor$^{T-/-}$ littermates at embryonic stage e15 (-1), newborn (0), and between 1- to 6-weeks

were harvested and counted (n=3 to 6 for each age group). Throughout this manuscript, error bars will denote standard error of the mean (SEM) and the following symbols; *, $p<0.05$; **, $p<0.01$; ***, $p<0.001$ the statistical significance as determined by Student's t test. **E**. Thymocytes from wild-type and rictor-deficient littermates were counted and stained for CD4, CD8α, TCRβ, CD25 and CD44 expression, followed by flow cytometric analysis of the DN subpopulation (gating the $CD4^{-}CD8^{-}$ cells). The proportion of each DN subset is indicated in the respective quadrant of a representative analysis. The relative numbers of DN2 -DN4 cells found in $rictor^{T+/+}$ and $rictor^{T-/-}$ littermates were plotted (n=9). **F**. The absolute numbers of each DN subset were determined by multiplying their relative numbers by the total amount of thymocytes (n=9). **G.** Thymocytes were stained for TCRβ, CD8α, CD4 and CD147 or CD127 expression and analyzed by flow cytometer. To distinguish CD8-ISP ($TCR\beta^{low}$) from lineage committed CD8-SP ($TCR\beta^{high}$) thymocytes, we gated for $TCR\beta^{low}$, $CD147^{+}$ among the $CD8^{+}CD4^{-}$ cells. Shown is a representative plot out of seven independent experiments. The absolute numbers of CD8-ISP cells were determined by multiplying their relative numbers by the total amount of thymocytes. **H**. Thymocytes were harvested from age-matched wild-type and $rictor^{T-/-}$ littermates at embryonic stage e15 (-1), newborn (0), as well as 3 and 4-weeks of age, stained for CD4, CD8α, TCRβ, and CD147 and analyzed by flow cytometry (n= 3 to 4 for each age group).

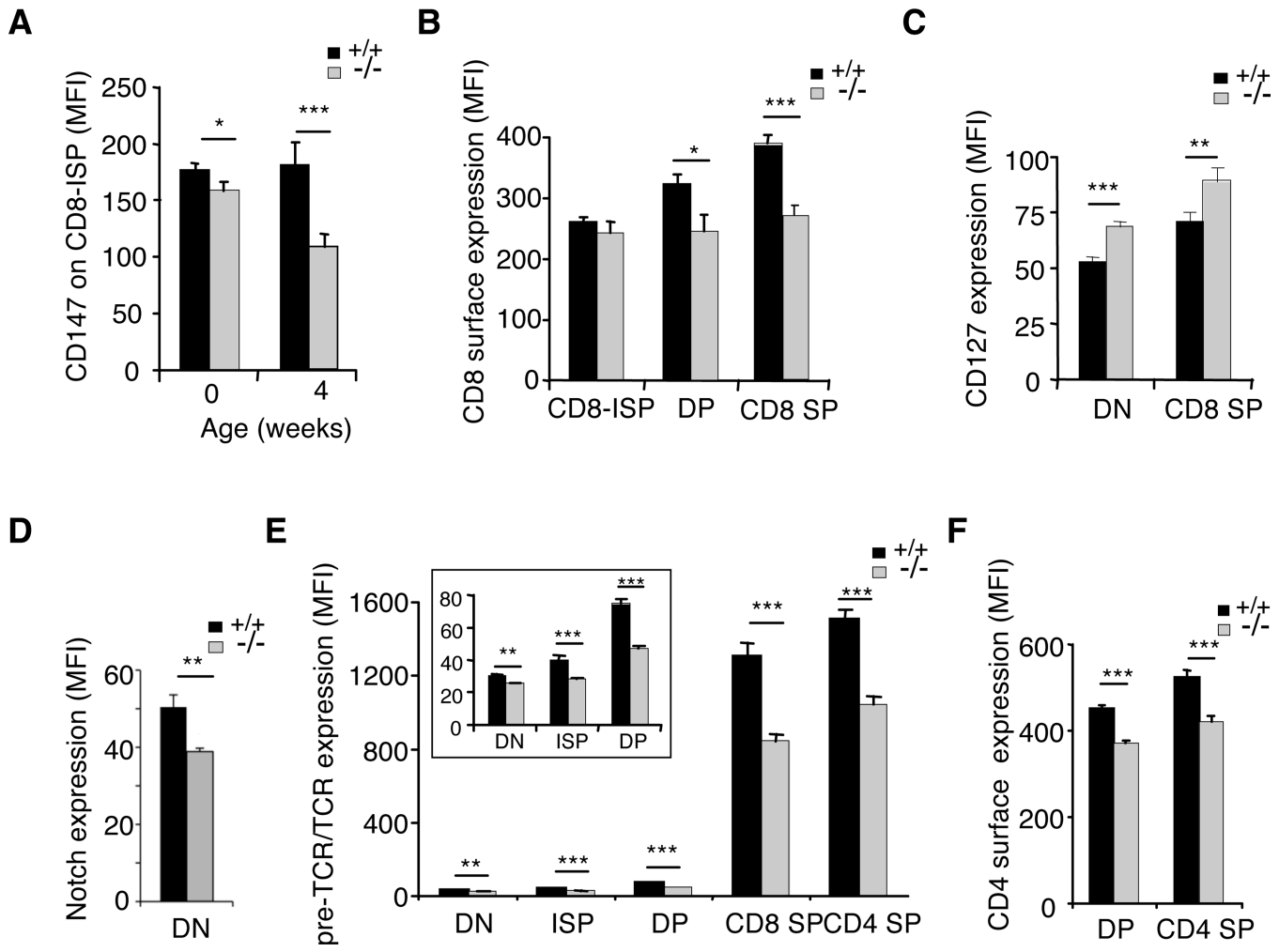

Figure 2. Rictor-deficiency caused defective receptor surface expression

Thymocytes were harvested from wild-type (+/+) and rictor-deficient (−/−) mice, stained for CD4, CD8α, TCRβ, as well as CD147 or CD127, followed by flow cytometric analysis. **A**. The mean fluorescence intensity (MFI) of CD147 expression on the surface of CD8-ISP cells was plotted for newborn (n=3) and 4-week-old (n=4) wild-type and rictor$^{T-/-}$ littermates. CD8-ISP thymocytes were defined as the TCRβ^{low}CD147^{+} subsets among CD8α^{+}CD4^{-} cells. **B**. MFI of CD8 expressed on CD8-ISP, CD8CD4 DP & CD8 SP (n=4). **C**. MFI of CD127 expressed on DN and CD8 SP thymocytes (n=4). **D.** MFI of Notch expressed on DN cells (n=4). **E**. MFI of pre-TCR or TCR expression was measured and plotted for all developmental stages (n=9). The inset represents a magnified plot of the receptors on DN to DP cells. **F**. MFI of CD4 expressed on DP & CD4 SP (n=4).

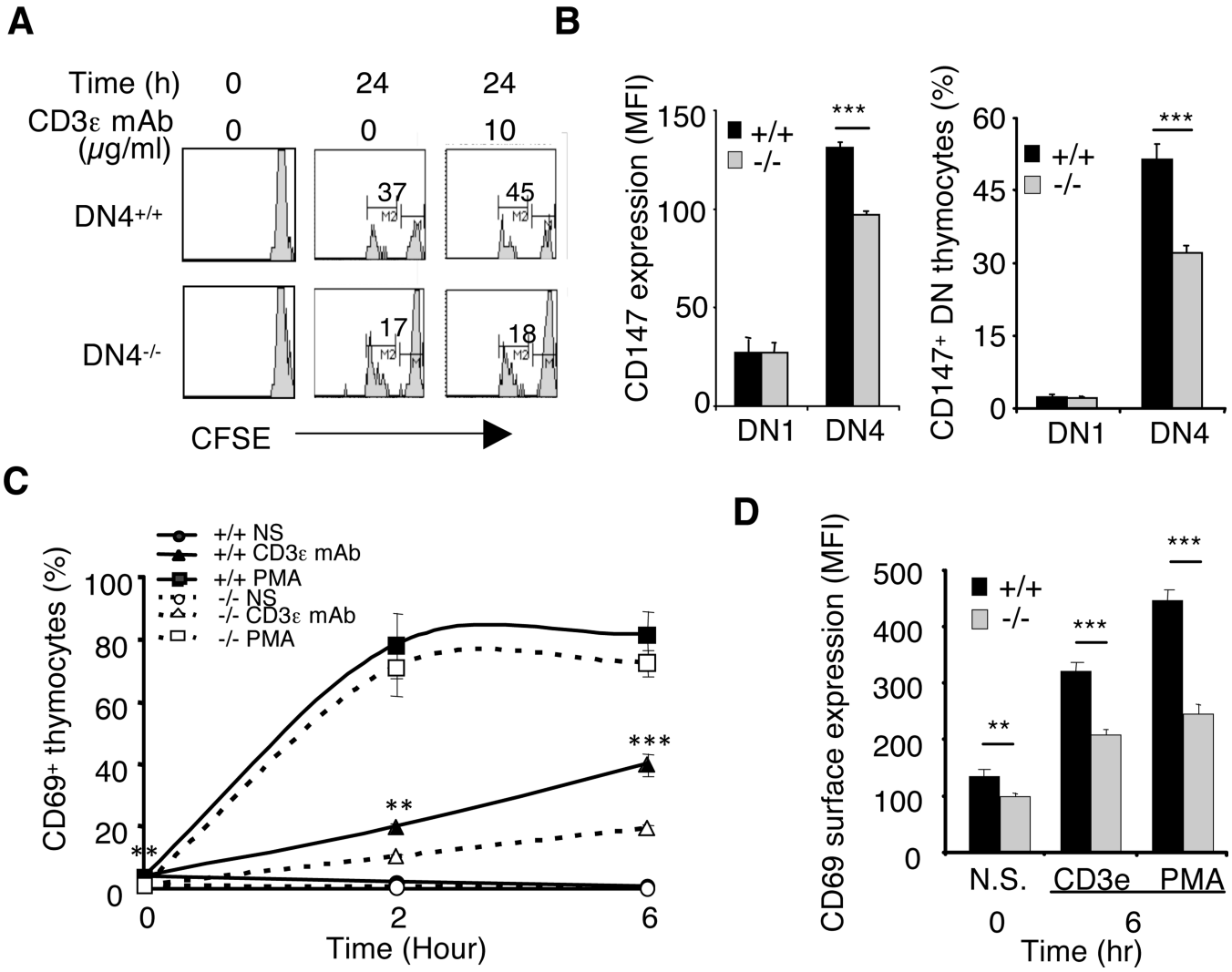

Figure 3. Rictor-deficiency caused suboptimal proliferation and cell activation

A. Rictor$^{T+/+}$ and rictor$^{T-/-}$ thymocytes were labeled with CFSE and cultured *ex vivo* for 24 hrs with or without 10 μg/ml of anti-CD3ε mAb. Cells were stained for TCRβ, CD4, and CD8β prior to measuring the fluorescence of CFSE in DN cells. The intensity of fluorescence decreases with each round of cell division. Shown is a representative experiment out of three. **B**. Thymocytes were stained for TCRβ, CD4, CD8, CD25, CD44 and CD147 and the relative number of CD147$^+$ cells as well as the MFI of CD147 was analyzed by flow cytometry (n=5). **C.** Thymocytes were cultured ex vivo in presence or absence of 10 μg/ml of anti-CD3ε mAb or 16 nM PMA for the indicated times, stained and the relative number of DP cells expressing CD69 was analyzed by flow cytometry (n= 3). **D**. MFI of CD69 upregulation in response to 6 hrs anti-CD3ε mAb (10 μg/ml) or PMA (16 nM) treatment (n= 3).

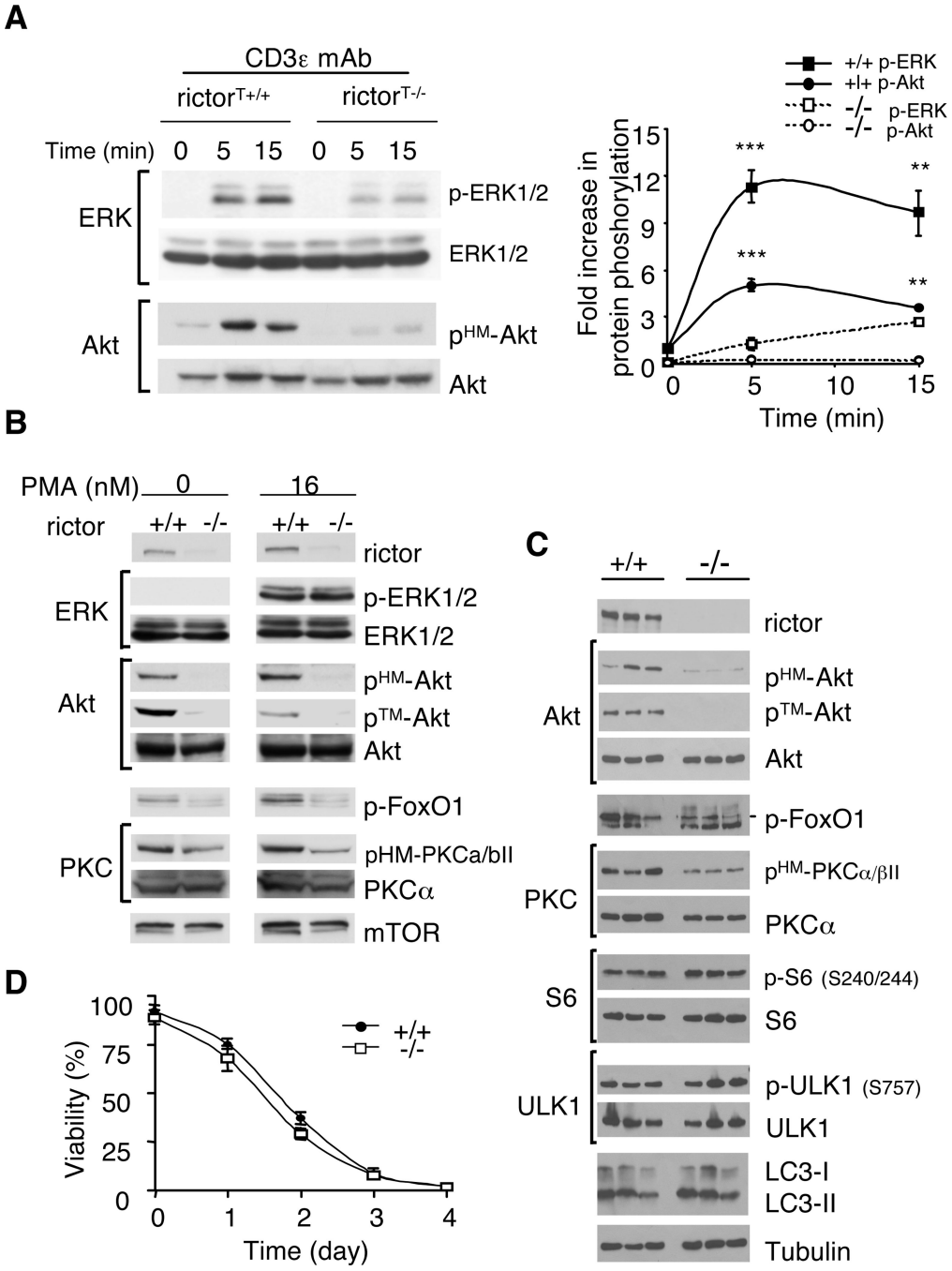

Figure 4. Rictor-deficiency caused suboptimal TCR signaling

A. Rictor$^{T+/+}$ and rictor$^{T-/-}$ DP thymocytes were stimulated in vitro for the indicated times with 10 μg/mL CD3ε mAb. Phosphorylation of ERK (T202/Y204) as well as the HM of Akt (S473) was analyzed by immunoblotting with the specific phospho-antibodies and quantitated by densitometry. Membranes were stripped and reblotted with sera against the native form of the respective kinases. Shown is a representative experiment out of three as well as a quantitative plot of fold increase of protein phosphorylation as compared to the non-stimulated kinases from wild-type cells (n= 3). **B**. Thymocytes were stimulated for 10

min with PMA (16 nM) and lysates were subjected to immunoblotting. Shown are representative blots of three experiments. **C.** Thymocytes of 3 rictor$^{T+/+}$ and 3 rictor$^{T-/-}$ littermates were harvested, counted and lysates were resolved by immunoblotting. Shown are representative blots of three experiments. **D**. Thymocytes were cultured, *ex vivo* at 37 ° C for 1 to 4 days. Following cell staining with Annexin V and propidium iodide (PI), viability was measured at various time points by flow cytometric analysis (n=4).

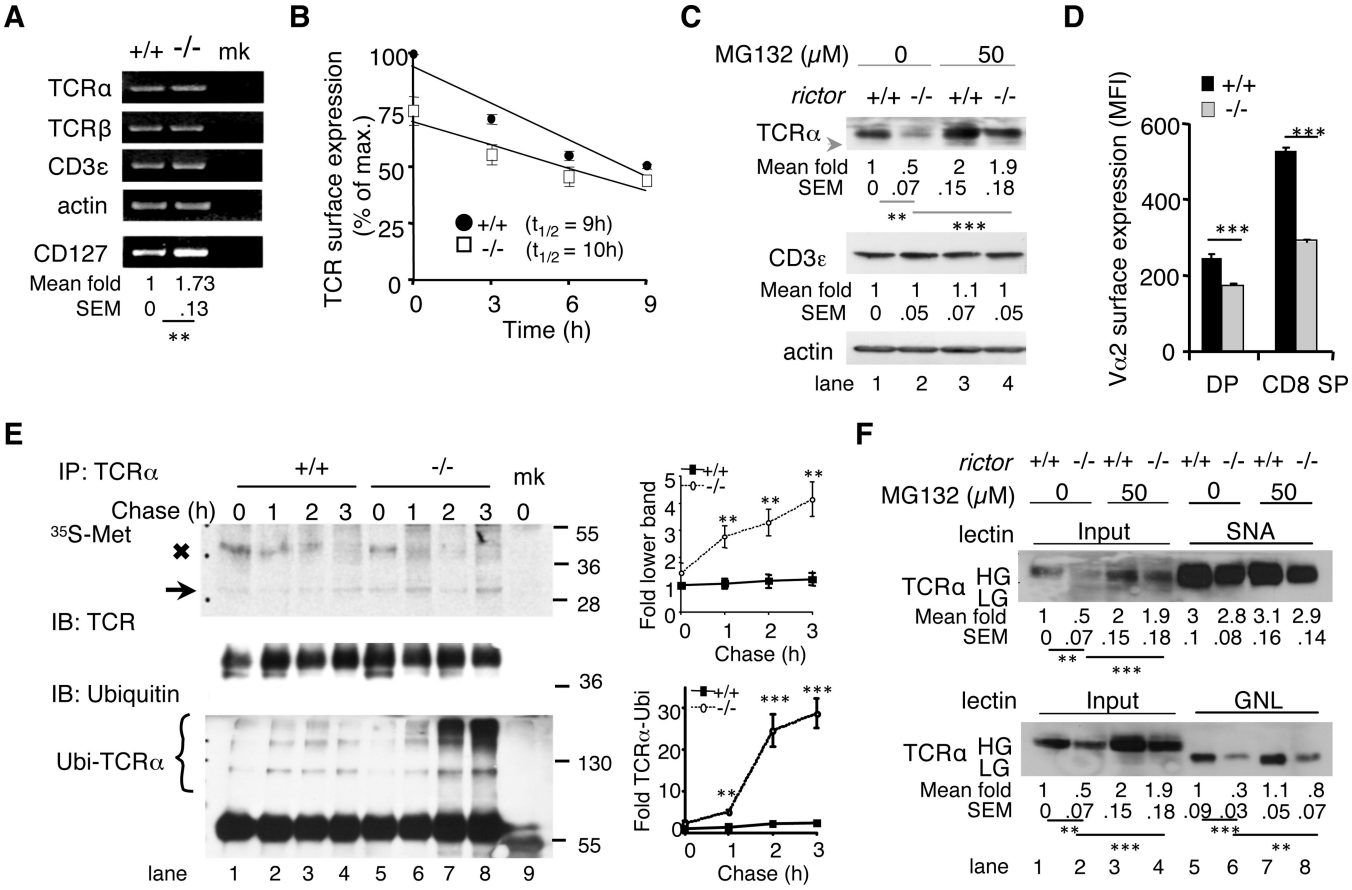

Figure 5. Rictor-deficiency caused defective processing of αβTCR

A. RNA was extracted from wild-type (+/+) and rictor-deficient (−/−) thymocytes and the mRNA expression of TCRα, TCRβ, CD3ε and CD127 was analyzed by RT-PCR and normalized to the expression of β-actin using the Image J software. (mk = mock amplification). The means and SEM of CD127 fold changes as compared to the expression in wild-type cells were indicated. Shown is a representative experiment out of three. **B**. Thymocytes were cultured *ex vivo* in presence of 100 μM cycloheximide for the indicated times and the amount of TCR was assessed by flow cytometric analysis and plotted as relative to the expression on the surface of wild-type cells (+/+) at the start of the experiment (100%). $T_{1/2}$ = 50% reduction of TCR surface expression (n=3). **C**. Thymocytes were treated with or without MG132 and total protein expression was analyzed in whole cell lysates. The arrow indicates low glycosylated, immature TCRα. The means and SEM of fold changes as compared to protein expressions in untreated wild-type cells (lane 1) were indicated below each blot. Shown are representative blots of five independent experiments. **D**. Thymocytes from 6-week-old wild-type and rictor-deficient OT-1/Rag-$2^{-/-}$ littermates were stained for CD4, CD8α, Vα2 (TCR–α) and Vβ5 (TCR–β) followed by flow cytometric analysis of Vα2 expression (MFI) on the surface of DP and CD8 SP cells (n=3). **E**. OT-1/rictor$^{T+/+}$ and OT-1/rictor$^{T-/-}$ thymocytes were subjected to pulse-chase labeling. Labeled immunoprecipitated TCRα-chains were visualized by autoradiography, while the amounts and ubiquitylation of IPed TCRα were assessed by immunoblotting (mk: mock IP). The arrow indicates the faster migrating TCRα-band. Molecular weights (kDa) are indicated on

the right. Shown is a representative of four experiments as well as quantitative plots (mean & SEM) of fold changes of the faster migrating TCRα (lower band) and TCR-ubiquitylation as compared to wild-type cells at the start of the pulse-chase (lane 1). The radioactive input was identical for all samples (not shown). **F**. Thymocytes were harvested from OT-1/Rag-$2^{-/-}$/rictor$^{T+/+}$ and OT-1/Rag-$2^{-/-}$/rictor$^{T-/-}$ mice and treated with vehicle or MG132. Lysates were subjected to SNA-agarose or GNL-agarose pull down assay followed by immunoblotting. The means and SEM of fold changes as compared to TCRα expression in untreated wild-type cells (lane 1) were indicated below each blot. Shown is a representative experiment out of three.

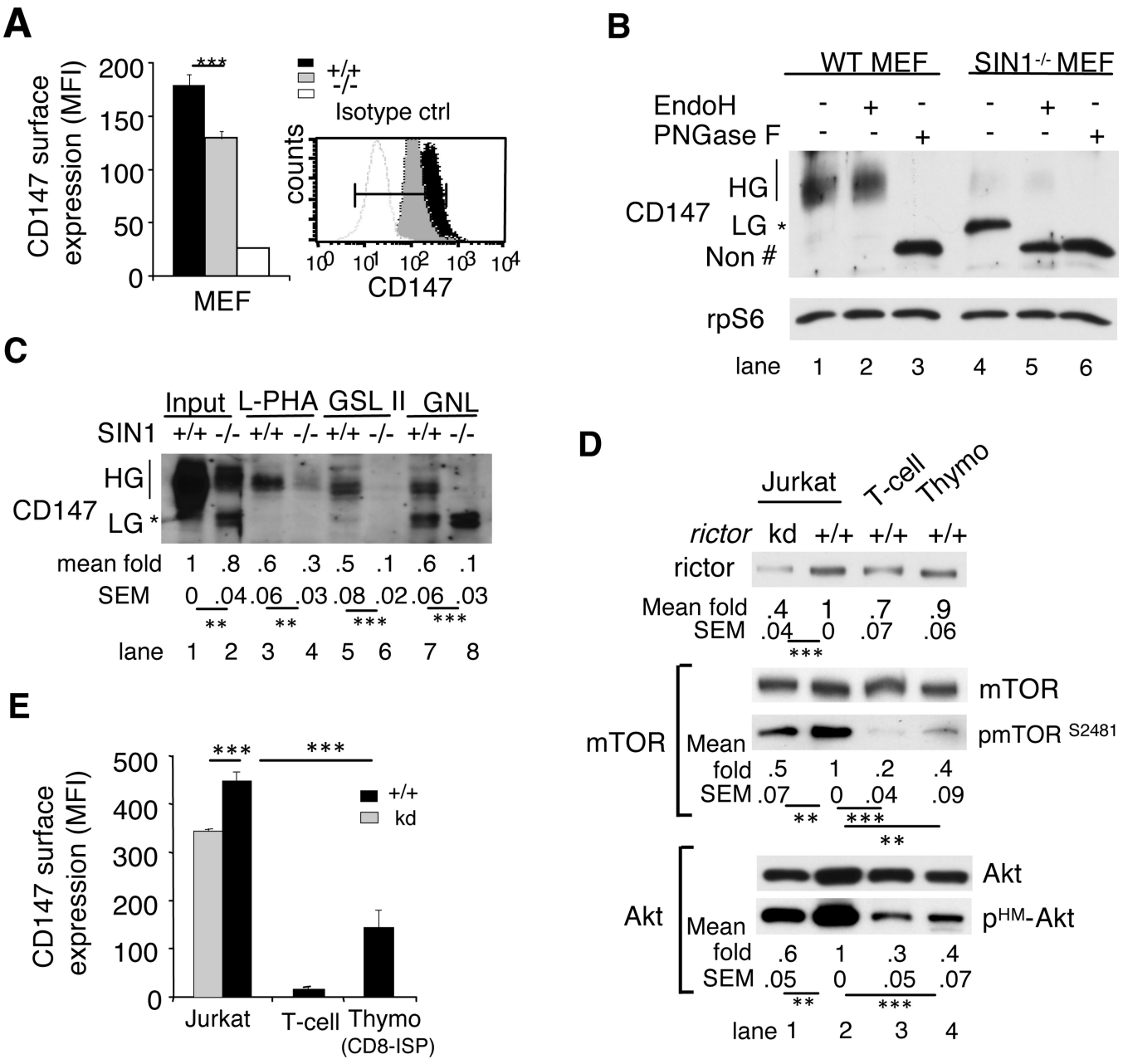

Figure 6. mTORC2 disruption diminished CD147 expression on the surface of mouse embryonic fibroblasts or immortalized T-cells

A. Wild-type (+/+) and SIN1-deficient (−/−) MEFs were harvested, stained for CD147 and propidium iodide (PI) followed by flow cytometric analysis of live cells (PI^{-}). MFI of CD147 was plotted from 4 distinct experiments. **B**. Lysates of wild-type and SIN1-deficient MEFs were incubated for 1 hr in presence or absence of glycosidases followed by CD147 immunoblotting. High (HG) or low (LG) glycosylated or non-*N*-glycosylated (Non #) CD147 forms are indicated. Shown is a representative experiment out of three **C**. Lysates from MEFs were subjected to pull down assays with the indicated lectin agaroses. The means and SEM of fold changes of CD147 HG as compared to the expression in wild-type cells (lane 1) were indicated below each blot. Shown is a representative experiment out of

three. **D**-**E.** Jurkat T-cells were transfected with rictor (kd) or scrambled (+/+) shRNAs. Jurkat cells, peripheral T-cells and thymocytes were (**D**) lysed and the phosphorylation and total protein expression were analyzed by immunoblotting. The mean and SEM of fold changes as compared to protein expressions in wild-type Jurkat cells (lane 2) were indicated below each blot. Shown is a representative experiment out of four, or (**E**) Cells were stained for TCRβ, and CD147 expression followed by flow cytometric analysis (n= 4).